Study of Biogenic and α,ω-Polyamines by Combined Inelastic Neutron Scattering and Raman Spectroscopies and by Ab Initio Molecular Orbital Calculations

M. Paula M. Marques,*,†,‡ Luís A. E. Batista de Carvalho,‡ and John Tomkinson§

Unidade I&D "Química-Física Molecular", Faculdade de Ciências e Tecnologia, Universidade de Coimbra, P-3049 Coimbra, Portugal, Dep. Bioquímica, Faculdade de Ciências e Tecnologia, Universidade de Coimbra, P-3049 Coimbra, Portugal, and ISIS Facility, The Rutherford Appleton Laboratory, Chilton, United Kingdom

Received: September 17, 2001; In Final Form: December 13, 2001

A study of the biogenic polyamines spermidine and spermine, as well as of the diamines $H_2N(CH_2)_nNH_2$ ($n = 2-10$ and $n = 12$), was carried out by both inelastic neutron scattering (INS) and Raman spectroscopies, for both their undeuterated and N-deuterated forms. Ab initio density functional theory (DFT) methods were also used, to obtain the calculated vibrational spectra of those molecules. A thorough vibrational analysis was performed, leading to the assignment of the solid-state spectra, both Raman and INS, of the polyamines studied, comprising all their longitudinal acoustic modes (LAM's).

1. Introduction

Polyamines are found in millimolar concentrations in most living cells (where they result from the decarboxylation of basic amino acids). They are intrinsic polycations essential for cell growth and differentiation.[1−6] In particular, putrescine (1,4-diaminobutane, $H_2N(CH_2)_4NH_2$), which is the first biogenic amine in the polyamine pathway, biosynthesised from arginine and the precursor of spermidine ($H_2N(CH_2)_3NH(CH_2)_4NH_2$) and spermine ($H_2N(CH_2)_3NH(CH_2)_4NH(CH_2)_3NH_2$), is widely distributed in both prokaryotic and eukaryotic cells. On account of absolute polyamine requirement for cell growth, interference with polyamine biosynthesis can be a rather promising therapeutical approach against proliferative diseases. In fact, an increased rate of those biosynthetic reactions has been unequivocally demonstrated in malignant processes.[7−11] Also, deregulated polyamine biosynthesis is a well recognized characteristic of animal and human cancers.[12] Moreover, it was verified that linkage of some of these molecules to previously tested anticancer drugs leads to a higher cytotoxic effect[13] and, in some cases, even to an enhancement of the efficacy of the long used first-generation drug cisplatin (*cis*-diaminedichloroplatinum(II)). The antitumor effect of polyamines and some of their metal complexes (e.g. Pt(II) or Pd(II)) is thought to be due to DNA rearrangements induced by binding of these compounds, which is strongly conformation dependent. However, the exact nature of the biochemical mechanisms underlying this biological activity is still unknown.

The conformational preferences of alkylamines depend on different factors, from steric, dipolar, and hyperconjugative effects to the relative importance of intra- vs intermolecular interactions, namely hydrogen-bond type close contacts, which were shown to have a determinant stabilizing role in linear amines.[14−16] There is presently no published work, at a molecular level, leading to a knowledge of the structure−activity relationship of such biologically relevant molecules. However, this would be of the utmost importance for understanding the biochemical mechanisms through which they act in living organisms, either in the regulation of normal cell growth and differentiation or in the cytotoxic effect of third-generation polyamine-derived anticancer drugs. Apart from a Raman and IR study reported on spermidine and spermine interactions with hydrochloric and phosphoric acids,[17] only a preliminary assignment of the Raman spectrum of putrescine (in aqueous solution) is available.[18] A conformational analysis of the small, linear amines 1,2-diaminoethane,[19] 1,3-diaminopropane,[20] and 1,4-diaminobutane (putrescine)[21] by either ab initio calculations or Raman spectroscopy, will prove very useful as a model in the present study of the larger analogues.

INS is a well suited technique for the study of hydrogenous material. Indeed, since neutrons have a mass similar to that of the hydrogen atom, an inelastic collision between them involves a significant transfer of both momentum, Q (Å^{-1}) and energy to the irradiated sample. The scattering cross-section, σ, which is a characteristic of each element and does not depend on its chemical environment, is 80 barns for hydrogen as opposed to 5 barns for most other elements. Therefore, the modes involving a significant hydrogen displacement will dominate the spectrum. The intensity of each molecular vibrational transition (I_i) follows the equation

$$I_i \propto Q^2 U_i^2 \exp(-Q^2 U_{\text{total}}^2)\sigma \qquad (1)$$

where, for each vibrational mode, i, U_i stands for the amplitude of vibration of the atoms in this mode and U_{total} represents the total amplitude of the atom in all the modes. The exponential term, $\exp(-Q^2U_{\text{total}}^2)$ is the well-known Debye−Waller factor, and to reduce its impact on the observed intensity the samples are cooled below 50 K.

The LAM's n (longitudinal acoustic modes with n nodes) are low-frequency modes detected between ca. 50 and 600 cm^{-1}, corresponding to in-plane expansions or contractions of all the CCC and CCN bond angles. The full longitudinal acoustic mode INS spectrum of a linear alkane was first determined for octadecane[22] and the whole set of LAM's for the 5−25 *n*-alkanes have been recently observed and assigned.[23] The spectral region

† Dep. Bioquímica, Universidade de Coimbra.
‡ Unidade I&D "Química-Física Molecular", Universidade de Coimbra.
§ The Rutherford Appleton Laboratory.

10.1021/jp013553k CCC: $22.00
Published on Web 02/21/2002

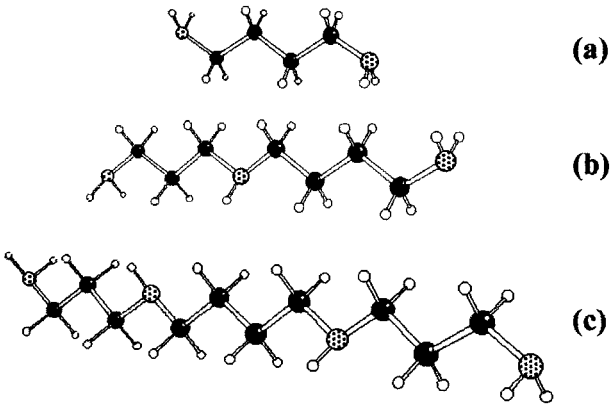

Figure 1. Schematic representation of the all-trans conformations of some of the polyamines studied in this work: (a) 1,4-diaminobutane; (b) spermidine; (c) spermine.

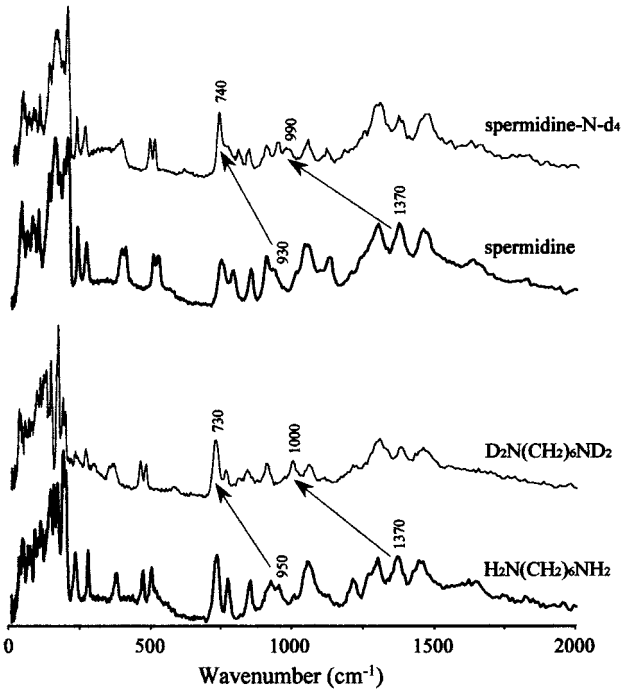

Figure 2. Experimental INS spectra (16−2000 cm^{-1}, at 20 K) for two distinct polyamines, in their undeuterated and N-deuterated forms.

below ca. 200 cm^{-1} contains mainly out-of-plane tranverse acoustic modes (TAM's), which will not be discussed in this work.

In the present work, a study of the homologous series of α,ω-diamines ($H_2N(CH_2)_nNH_2$) ($n = 2-10$ and $n = 12$), as well as of the polyamines spermidine ($H_2N(CH_2)_3NH(CH_2)_4NH_2$) and spermine ($H_2N(CH_2)_3NH(CH_2)_4NH(CH_2)_3NH_2$), was undertaken by vibrational spectroscopy (Raman and INS) combined with ab initio DFT calculations. The N-deuterated forms of those molecules were also studied.

2. Experimental Section

2.1. INS Spectroscopy. The INS spectra were obtained in the Rutherford Appleton Laboratory (Chilton, United Kingdom), at the ISIS pulsed neutron source on the TOSCA spectrometer. This is an indirect geometry time-of-flight, high-resolution (($\Delta E/E$) ca. 2%), broad range spectrometer (more details are available elsewhere[24]). Solid compounds (2−3 g each) were wrapped in aluminum foil, while the liquids were placed in thin-walled aluminum cans, which filled the beam. The samples were cooled to ca. 20 K. Data were recorded in the energy range 16−4000 cm^{-1} and converted to the conventional scattering law, $S(Q,\nu)$, vs energy tranfer (in cm^{-1}) through standard programs.

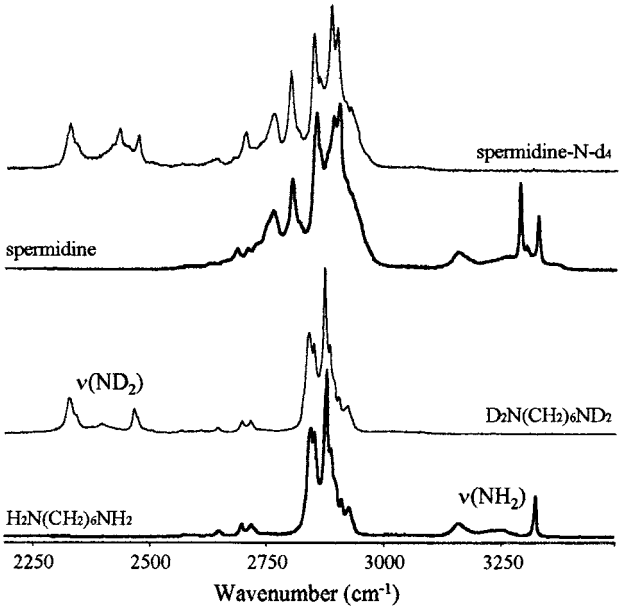

Figure 3. Experimental Raman spectra (2200−3500 cm^{-1}) for two distinct polyamines (in the solid state), in their undeuterated and N-deuterated forms.

TABLE 1: Experimental and Calculated Wavenumbers (cm^{-1}) for 1,2-Diaminoethane (C_{2h}) in the Low-Frequency Region

experimental		calculated (all-trans conformer)[a]				approximate description
Raman[d]	INS	Raman[b]	infrared[c]	INS	sym species	
			1,2-Diaminoethane			
548	522					NH_2 torsion (H-bonded)
486						
470	474	457(8)		457	A_g	in-plane CCN deformation (LAM 1)
430	432	321(5)		321	B_g	NH_2 torsion
	409		283 (120)	282	A_u	NH_2 torsion
	359					
	314		270 (19)	270	B_u	in-plane CCN deformation (LAM 2)
	207		145 (0)	145	A_u	out-of-plane CCN deformation (TAM)
177	180					
150	~150					
129	130					
102	105					
88	85					
	75					
			1,2-Diaminoethane-*N*-d_4			
493						
443						
436	439	412(6)		411	A_g	in-plane CCN deformation (LAM 1)
436						
	317		250 (19)	249	B_u	in-plane CCN deformation (LAM 2)
~280	365	248(2)		249	B_g	ND_2 torsion
			208 (63)	208	A_u	ND_2 torsion
220	217					
182	189					
	175					
	148					
143	142					
	132		132 (1)	132	A_u	out-of-plane CCN deformation (TAM)
	126					
108	118					
99						
78	70					

[a] B3LYP/6-31G* level of calculation. [b] Raman scattering activities in Å·amu^{-1}. [c] IR intensities in km·mol^{-1}. [d] Reference 19.

TABLE 2: Experimental and Calculated Wavenumbers (cm^{-1}) for 1,3-Diaminopropane (C_{2v}) in the Low-Frequency Region

experimental		calculated (all-trans conformer)[a]				approximate description
Raman	INS	Raman[b]	infrared[c]	INS	sym species	
			1,3-Diaminopropane			
	527					NH_2 torsion (H-bonded)
	465	444 (1)	444 (15)	444	B_2	in-plane CCN deformation (LAM 2)
		301 (5)		301	A_2	NH_2 torsion
432		300 (1)	300 (105)	301	B1	
423	409	397 (10)		397	A_1	in-plane CCN deformation (LAM 1)
~250	248	183 (1)	183 (4)	183	A_1	in-plane CCN deformation (LAM 3)
218						
201						
	191	126 (0)	126 (0)	125	A_2	out-of-plane CCN deformation (TAM)
180	180					
	174		119 (5)	120	B_1	out-of-plane CCN deformation (TAM)
	150					
137	134					
124	120					
	101					
92	87					
82	77					
			1,3-Diaminopropane-*N*-d_4			
	428	406 (1)		405	B_2	in-plane CCN deformation (LAM 2)
411			406 (25)			
	406	375 (8)		375	A_1	in-plane CCN deformation (LAM 1)
324		235 (2)		232	A_2	ND_2 torsion
			230 (51)	232	B_1	ND_2 torsion
~235	*d*	171 (1)	171 (3)	171	A_1	in-plane CCN deformation (LAM 3)
211						
191	*d*		115 (5)	112	B_1	out-of-plane CCN deformation (TAM)
172	*d*	110 (0)	110 (0)	112	A_2	out-of-plane CCN deformation (TAM)
139	141					
124						
92						
80						
59						

[a] B3LYP/6-31G* level of calculation. [b] Raman scattering activities in Å·amu^{-1}. [c] IR intensities in km·mol^{-1}. [d] Not observed due to glassy nature of the sample.

2.2. Raman Spectroscopy. The Raman spectra performed at room temperature were obtained on a Spex Ramalog 1403 double spectrometer (focal distance 0.85 m, aperture *f*/7.8) equipped with holographic gratings of 1800 grooves·mm^{-1} and a detector assembly containing a thermoelectrically cooled Hamamatsu R928 photomultiplier tube. The spectrometer operated with slits of 320 μm and 1 cm^{-1} s^{-1}. Below room temperature (ca. 220 K), a homemade Harney-Miller type assembly was used, in a triple monochromator Jobin-Yvon T64000 Raman system (0.640 m, *f*/7.5) with holographic gratings of 1800 grooves·mm^{-1}. The detection system was a nonintensified CCD (Charge Coupled Device) and the entrance slit was set to 300 μm.

The 514.5 nm line of an Ar^+ laser (Coherent, model Innova 300) was used as excitation radiation, providing 100−120 mW at the sample position. Samples were sealed in Kimax glass capillary tubes of 0.8 mm inner diameter. Under the above-mentioned conditions, the error in wavenumbers was estimated to be within 1 cm^{-1}.

2.3. Ab Initio MO Calculations. The ab initio calculations were carried out with the GAUSSIAN 98W program,[25] within the density functional theory (DFT) approach, using the B3LYP method,[26−31] which includes a mixture of Hartree-Fock (HF) and DFT exchange terms. The gradient-corrected correlation functional was used[32,33] (parametrized after Becke[34,35]), along with the double-ζ split valence basis sets 6-31G*[36] and 6-31G**.[36,37]

Only the geometries with all skeletal dihedral angles equal to 180° (all-trans) were considered in the present work. Molecular geometries were fully optimized by the Berny algorithm, using redundant internal coordinates:[38] the bond lengths to within ca. 0.1 pm and the bond angles to within ca. 0.1°. The final root-mean-square (rms) gradients were always less than 3×10^{-4} Hartree·bohr^{-1} or Hartree·radian^{-1}.

The calculated INS transition intensities were obtained as previously reported,[23] using a program written by Chris Middleton, of Syracuse University, Syracuse, NY. The bandwidths of the calculated spectra were adjusted by inspection, on a sample by sample basis, to provide the best agreement with the experimental data.

TABLE 3: Experimental and Calculated Wavenumbers (cm^{-1}) for 1,4-Diaminobutane (Putrescine) (C_{2h}) in the Low-Frequency Region

experimental		calculated (all-trans conformer)[a]				approximate description
Raman	INS	Raman[b]	infrared[c]	INS	sym species	
			1,4-Diaminobutane			
	571					
	530					NH_2 torsion (H-bonded)
	517		506 (11)	506	B_u	in-plane CCN deformation (LAM 2)
417		306 (6)		311	B_g	NH_2 torsion
368	364	351 (4)		351	A_g	in-plane CCN deformation (LAM 1)
352	354	327 (7)		325	A_g	in-plane CCN deformation (LAM 3)
			314 (104)	311	A_u	NH_2 torsion
198	199					
	191	165 (0)		164	B_g	out-of-plane CCN deformation (TAM)
	177		130 (6)	130	B_u	in-plane CCN deformation (LAM 4)
157	158					
	143					
	132		103 (11)	103	A_u	out-of-plane CCN deformation (TAM)
	112		79 (1)	79	A_u	out-of-plane CCN deformation (TAM)
	85					
	65					
	53					
			1,4-Diaminobutane-*N*-d_4			
	486		468 (23)	468	B_u	in-plane CCN deformation (LAM 2)
359	359	349 (4)		352	A_g	in-plane CCN deformation (LAM 1)
340						
324	319	296 (6)		296	A_g	in-plane CCN deformation (LAM 3)
			243 (49)	242	A_u	ND_2 torsion
289		232 (3)		232	B_g	ND_2 torsion
	189	159 (0)		159	B_g	out-of-plane CCN deformation (TAM)
	169		124 (6)	124	B_u	in-plane CCN deformation (LAM 4)
160	150					
	126		95 (12)	95	A_u	out-of-plane CCN deformation (TAM)
110						
	106		74 (0)	74	A_u	out-of-plane CCN deformation (TAM)
95						
	81					
	63					
	51					

[a] B3LYP/6-31G* level of calculation. [b] Raman scattering activities in Å·amu^{-1}. [c] IR intensities in km·mol^{-1}.

TABLE 4: Experimental and Calculated Wavenumbers (cm^{-1}) for 1,5-Diaminopentane (Cadaverine) (C_{2v}) in the Low-Frequency Region

experimental		calculated (all-trans conformer)[a]				approximate description
Raman	INS	Raman[b]	infrared[c]	INS	sym species	
			1,5-Diaminopentane			
	530					NH_2 torsion (H-bonded)
	504		501 (3)	501	B_2	in-plane CCN deformation (LAM 2)
460	454	443 (1)	443 (4)	443	A_1	in-plane CCN deformation (LAM 3)
		301 (1)	301 (105)	300	B_1	NH_2 torsion
418		300 (5)		300	A_2	NH_2 torsion
326	315	301 (10)		300	A_1	in-plane CCN deformation (LAM 1)
313	290		255 (7)	255	B_2	in-plane CCN deformation (LAM 4)
183	189		162 (3)	162	B_1	out-of-plane CCN deformation (TAM)
177	167	149 (0)	149 (0)	150	A_2	out-of-plane CCN deformation (TAM)
	144		99 (2)	99	A_1	in-plane CCN deformation (LAM 5)
	134	89 (0)	89 (0)	89	A_2	out-of-plane CCN deformation (TAM)
108	111		68 (3)	68	B_1	out-of-plane CCN deformation (TAM)
102	99					
	89					
	75					
	48					
			1,5-Diaminopentane-*N*-d_4			
477	483		474 (11)	474	B_2	in-plane CCN deformation (LAM 2)
	438	422 (1)	422 (3)	422	A_1	in-plane CCN deformation (LAM 3)
320	301	287 (9)		287	A_1	in-plane CCN deformation (LAM 1)
	278		243 (9)	242	B_2	in-plane CCN deformation (LAM 4)
			233 (49)	232	B_1	ND_2 torsion
		231 (2)		232	A_2	ND_2 torsion
			154 (5)	153	B_1	out-of-plane CCN deformation (TAM)
179	183	146 (0)	146 (0)	147	A_2	out-of-plane CCN deformation (TAM)
	142		95 (2)	95	A_1	in-plane CCN deformation (LAM 5)
107	110					
102						
	88	80 (0)	80 (0)	80	A_2	out-of-plane CCN deformation (TAM)
	72		66 (3)	66	B_1	out-of-plane CCN deformation (TAM)

[a] B3LYP/6-31G* level of calculation. [b] Raman scattering activities in Å·amu^{-1}. [c] IR intensities in km·mol^{-1}.

2.4. Reagents. The polyamines were purchased from Sigma-Aldrich. The deuterated compounds were obtained by mixing the amines with D_2O (ca. 10% excess) and distilling under vacuum (this process being repeated at least three times). The solid amines were purified by sublimation, while the liquids were distilled under vacuum. All the samples being air or moisture sensitive, they were always handled in a glovebox under an argon atmosphere.

3. Results and Discussion

This kind of linear polyamine molecules can adopt different conformations, by varying the dihedral angles that determine their overall orientation. The most common geometries have skeletal dihedral angles near 60° (gauche), 180° (trans), and −60° (gauche′). Intramolecular (N)H···:N and (C)H···:N hydrogen bonds determine the conformational preferences of these compounds, as previously confirmed by both ab initio methods and Raman spectroscopy for molecules as liquids and aqueous solutes.[19−21] However, the crystal packing of the polyamines in the solid state, which corresponds to the present study, is

TABLE 5: Experimental and Calculated Wavenumbers (cm^{-1}) for Spermidine (C_1) in the Low-Frequency Region.

experimental		calculated (all-trans conformer)[a]			approximate description
Raman	INS	Raman[b]	infrared[c]	INS	
			Spermidine		
526	529	529 (2)	529 (1)	529	in-plane CCN deformation (LAM 3)
	513		507 (3)	507	in-plane CCN deformation (LAM 4)
408	414		407 (2)	407	in-plane CCN deformation (LAM 2)
382	400	385 (1)	385 (1)	385	in-plane CCN deformation (LAM 5)
		304 (2)	304 (59)	302	NH_2 torsion
∼370		301 (3)	301 (44)	302	NH_2 torsion
	277		252 (10)	252	in-plane CCN deformation (LAM 6)
240	246	228 (8)		228	in-plane CCN deformation (LAM 1)
	211		179 (2)	179	out-of-plane CCN deformation (TAM)
197	198		165 (5)	165	out-of-plane CCN deformation (TAM)
181	183		139 (2)	138	out-of-plane CCN deformation (TAM)
	∼168	137 (1)		138	in-plane CCN deformation (LAM 7)
149	146		116 (1)	116	out-of-plane CCN deformation (TAM)
131					
122		86 (0)	86 (0)	85	out-of-plane CCN deformation (TAM)
111	110		66 (6)	66	out-of-plane CCN deformation (TAM)
	97		52 (1)	52	in-plane CCN deformation (LAM 8)
	88	35 (0)	35 (0)	35	out-of-plane CCN deformation (TAM)
	70				
	57				
	50				
			Spermidine-*N*-d_5		
509	511	510 (1)	510 (1)	510	in-plane CCN deformation (LAM 3)
	494		489 (7)	489	in-plane CCN deformation (LAM 4)
397	395		388 (5)	388	in-plane CCN deformation (LAM 2)
	382	369 (1)	369 (1)	369	in-plane CCN deformation (LAM 5)
		234 (1)	234 (36)	233	ND_2 torsion
285		232 (2)	232 (11)	233	ND_2 torsion
274	267		243 (11)	242	in-plane CCN deformation (LAM 6)
233	239	222 (8)	222 (1)	223	in-plane CCN deformation (LAM 1)
	205		174 (1)	174	out-of-plane CCN deformation (TAM)
190	190		159 (7)	159	out-of-plane CCN deformation (TAM)
177	172		135 (2)	134	out-of-plane CCN deformation (TAM)
	163	132 (1)		134	in-plane CCN deformation (LAM 7)
148	143		108 (1)	108	out-of-plane CCN deformation (TAM)
130					
121		83 (0)	83 (0)	83	out-of-plane CCN deformation (TAM)
110	108		61 (6)	61	out-of-plane CCN deformation (TAM)
92	94		50 (1)	50	in-plane CCN deformation (LAM 8)
	86		33 (0)	33	out-of-plane CCN deformation (TAM)
	69				
	56				
	49				

[a] B3LYP/6-31G* level of calculation. [b] Raman scattering activities in Å·amu^{-1}. [c] IR intensities in km·mol^{-1}.

TABLE 6: Experimental and Calculated Wavenumbers (cm^{-1}) for Spermine (C_2) in the Low-Frequency Region

experimental		calculated (all-trans conformer)[a]			approximate description
Raman	INS	Raman[b]	infrared[c]	INS	
			Spermine		
			538 (3)	538	in-plane CCN deformation (LAM 4)
533	532	531 (1)	531 (1)	531	in-plane CCN deformation (LAM 5)
	496		491 (3)	491	in-plane CCN deformation (LAM 6)
446	443	443 (2)		443	in-plane CCN deformation (LAM 3)
418	413	403 (3)		403	in-plane CCN deformation (LAM 7)
	405				
			305 (103)	306	NH_2 torsion
~380		305 (5)	305 (1)	306	NH_2 torsion
	361				
	328	320 (0)	320 (0)	319	in-plane CCN deformation (LAM 2)
	317		307 (11)	306	in-plane CCN deformation (LAM 8)
247	247	221 (1)		221	in-plane CCN deformation (LAM 9)
	216				
	208		183 (3)	183	out-of-plane CCN deformation (TAM)
	197				
~200	190	174 (1)	174 (1)	174	out-of-plane CCN deformation (TAM)
182	176	168 (5)		169	in-plane CCN deformation (LAM 1)
		158 (1)	158 (4)	157	out-of-plane CCN deformation (TAM)
		157 (1)	157 (5)	157	out-of-plane CCN deformation (TAM)
	170				
	163	124 (0)	124 (0)	122	out-of-plane CCN deformation (TAM)
161	161		139 (2)	139	in-plane CCN deformation (LAM 10)
	155		121 (3)	122	out-of-plane CCN deformation (TAM)
140	140		87 (1)	86	out-of-plane CCN deformation (TAM)
	129		85 (1)	86	out-of-plane CCN deformation (TAM)
112	115	73 (0)	73 (0)	73	in-plane CCN deformation (LAM 11)
	96		54 (3)	54	out-of-plane CCN deformation (TAM)
	89				
85	85	46 (0)	46 (0)	46	out-of-plane CCN deformation (TAM)
		27 (0)	27 (0)	26	in-plane CCN deformation (LAM 12)
	78	21 (0)	21 (0)	21	out-of-plane CCN deformation (TAM)
69					
	60				
54	54				
	46				
			Spermine-*N*-d_6		
			527 (4)	527	in-plane CCN deformation (LAM 4)
520	522	518 (1)	518 (1)	518	in-plane CCN deformation (LAM 5)
	479		469 (9)	469	in-plane CCN deformation (LAM 6)
434	432	432 (2)		432	in-plane CCN deformation (LAM 3)
406					
396	398	384 (2)		384	in-plane CCN deformation (LAM 7)
	354				
			316 (2)	316	in-plane CCN deformation (LAM 2)
	318		295 (12)	295	in-plane CCN deformation (LAM 8)
~280		235 (3)		235	ND_2 torsion
			235 (48)	235	ND_2 torsion
~240	240	215 (0)	215 (0)	215	in-plane CCN deformation (LAM 9)
	206		178 (3)	177	out-of-plane CCN deformation (TAM)
	192				
~190	185	172 (1)	172 (2)	172	out-of-plane CCN deformation (TAM)
179	174	164 (5)		165	in-plane CCN deformation (LAM 1)
		151 (1)	151 (4)	151	out-of-plane CCN deformation (TAM)
		151 (1)	151 (4)	151	out-of-plane CCN deformation (TAM)
	168				
	162	122 (0)	122 (0)	122	out-of-plane CCN deformation (TAM)
156	158		135 (2)	135	in-plane CCN deformation (LAM 10)
	149		113 (4)	114	out-of-plane CCN deformation (TAM)
132	138		84 (1)	83	out-of-plane CCN deformation (TAM)
	125		82 (1)	83	out-of-plane CCN deformation (TAM)
111	114	71 (0)	71 (0)	71	in-plane CCN deformation (LAM 11)
	95		50 (3)	50	out-of-plane CCN deformation (TAM)
84	84	45 (0)	45 (0)	46	out-of-plane CCN deformation (TAM)
	75	26 (0)	26 (0)	26	in-plane CCN deformation (LAM 12)
		20 (0)	20 (0)	20	out-of-plane CCN deformation (TAM)
	60				
54	53				
43	46				

[a] B3LYP/6-31G* level of calculation. [b] Raman scattering activities in Å·amu^{-1}. [c] IR intensities in km·mol^{-1}.

not compatible with conformations displaying this kind of intramolecular close contacts. Thus, only the all-trans conformers (Figure 1) are expected to occur. Under these conditions the polyamines behave very much as saturated linear alkanes, for which the all-trans conformation has long been recognized as energetically the most favored.[39] Moreover, at physiological pH these amines are totally protonated, which renders them into

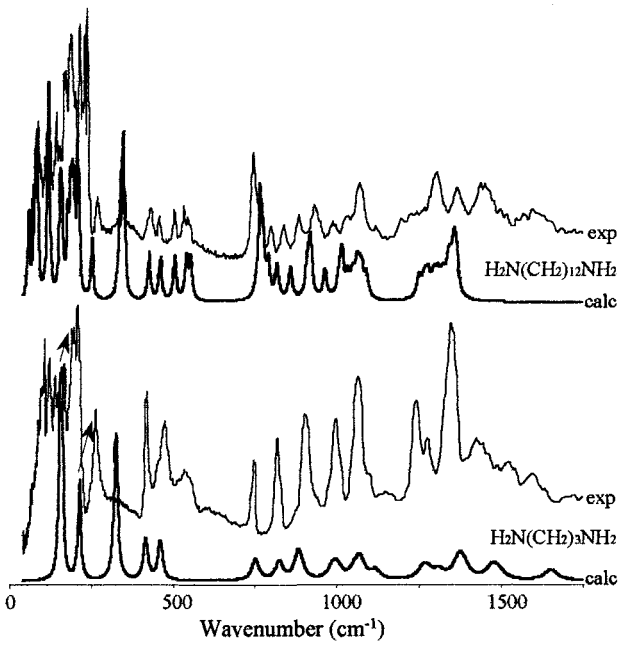

Figure 4. Experimental (20 K) and calculated (B3LYP/6-31G*) INS spectra (16−1750 cm^{-1}) for two different $H_2N(CH_2)_nNH_2$ diamines.

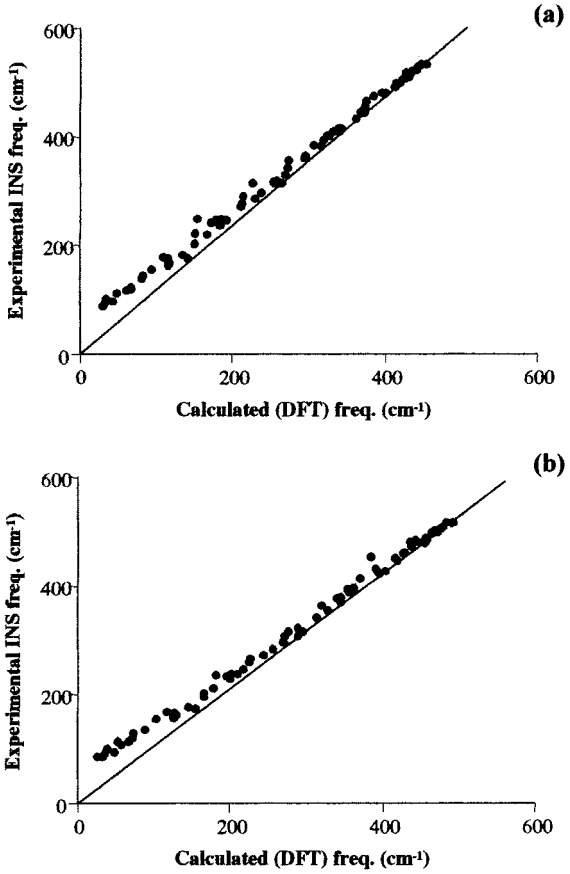

Figure 5. Plots of experimental vs calculated INS band center frequencies (LAM modes) for the series of polyamines studied ($H_2N(CH_2)_nNH_2$ ($n = 2-10$, $n = 12$), spermidine and spermine): (a) undeuterated; (b) N-deuterated. (Calculated values obtained at the B3LYP/6-31G* level. The lines correspond to a full accordance.)

polycationic species and hinders the formation of either (N)H···:N or (C)H···:N intramolecular contacts.

In the absence of intramolecular hydrogen-bond interactions in these totally extended amines, only three effects are relevant

TABLE 7: Longitudinal Acoustic Vibrational Modes (LAM's) for the $H_2N(CH_2)_nNH_2$ ($n = 2-10$, $n = 12$) Diamines, Spermidine and Spermine

			i										
N			1	2	3	4	5	6	7	8	9	10	11	12
4	1,2dae	exp (INS)	474	314										
	(C_2h)	exp (Raman)	470											
		calc[a]	457 (Ag)	270 (Bu)										
		κ	0.333	0.666										
5	1,3dap	exp (INS)	409	465	248									
	(C_2v)	exp (Raman)	423		250									
		calc	397 (A1)	444 (B2)	183 (A1)									
		κ	0.250	0.500	0.750									
6	1,4dab	exp (INS)	364	517	354	177								
	(C_2h)	exp (Raman)	368		352									
		calc	351 (Ag)	506 (Bu)	325 (Ag)	130 (Bu)								
		κ	0.200	0.400	0.600	0.800								
7	1,5dap	exp (INS)	315	504	454	290	144							
	(C_2v)	exp (Raman)	326		460	313								
		calc	300 (A1)	501 (B2)	443 (A1)	255 (B2)	99 (A1)							
		κ	0.167	0.333	0.500	0.667	0.833							
8	1,6dah	exp (INS)	284	477	506	383	240	123						
	(C_2h)	exp (Raman)	286		507									
		calc	272 (Ag)	472 (Bu)	505 (Ag)	365 (Bu)	204 (Ag)	80 (Bu)						
		κ	0.143	0.286	0.429	0.571	0.714	0.857						
9	1,7dah	exp (INS)	256	450	521	434	320	164	119					
	(C_2v)	exp (Raman)	269		525	438								
		calc	241 (A1)	449 (B2)	519 (A1)	428 (B2)	301 (A1)	163 (B2)	62 (A1)					
		κ	0.125	0.250	0.375	0.500	0.625	0.750	0.875					
10	1,8dao	exp (INS)	236	407	514	496	391	269	175	112				
	(C_2h)	exp (Raman)	236		517		397							
		calc	219 (Ag)	404 (Bu)	514 (Ag)	492 (Bu)	379 (Ag)	250 (Bu)	138 (Ag)	58 (Bu)				
		κ	0.111	0.222	0.333	0.444	0.555	0.666	0.777	0.888				
	spd	exp (INS)	246	414	529	513	400	277	168	97				
	(C_1)	exp (Raman)	240	408	526		382							
		calc	228	407	529	507	385	252	138	52				
		κ	0.111	0.222	0.333	0.444	0.555	0.666	0.777	0.888				
11	1,9dan	exp (INS)	218	382	498	519	445	341	246	156	100			
	(C_2v)	exp (Raman)	229	379	504	495	450		223		95			
		calc	199 (A1)	376 (B2)	498 (A1)	516 (B2)	437 (A1)	323 (B2)	211 (A1)	112 (B2)	42 (A1)			
		κ	0.100	0.200	0.300	0.400	0.500	0.600	0.700	0.800	0.900			
	1,10dad	exp (INS)	201	359	479	527	491	401	296	221	137	95		
	(C_2h)	exp (Raman)	201		476		489		297		132			
		calc	180 (Ag)	349 (Bu)	469 (Ag)	525 (Bu)	489 (Ag)	389 (Bu)	282 (Ag)	180 (Bu)	98 (Ag)	39 (Bu)		
		κ	0.091	0.182	0.273	0.364	0.455	0.545	0.636	0.727	0.818	0.909		
14	1,12dad	exp (INS)	181	314	432	509	522	479	407	314	237	167	118	87
	(C_2h)	exp (Raman)	175		433		522		408		239			
		calc	160 (Ag)	314 (Bu)	429 (Ag)	510 (Bu)	523 (Ag)	474 (Bu)	394 (Ag)	302 (Bu)	217 (Ag)	140 (Bu)	80 (Ag)	35 (Bu)
		κ	0.077	0.154	0.231	0.308	0.385	0.462	0.539	0.615	0.692	0.769	0.846	0.923
	sp	exp (INS)	176	328	443	532	532	496	413	317	247	161	115	
	(C_2)	exp (Raman)	182		446	533	533		418		247	161	112	78
		calc	169	319	443	538	531	491	403	306	221	139	73	26
		κ	0.077	0.154	0.231	0.308	0.385	0.462	0.539	0.615	0.692	0.769	0.846	0.923

[a] At the B3LYP/6-31G* level. $i = 1, 2, ..., (N - 2)$; $\kappa = i/(N - 1)$.

in determining conformation: intermolecular H-bonds and electrostatic and steric forces. The former are prone to be rather strong, given the linear geometry of our samples and the strong directional nature of the hydrogen bonds.[40,41]

Previously performed conformational studies on both small α,ω-diamines ($H_2N(CH_2)_nNH_2$, $n = 2-4$) and similar linear polyamines[19-21] allowed us to corroborate that the all-trans is the predominant or even the sole conformation for this kind of molecules in the solid state. These conformational preferences also apply to the larger spermidine (triamine) and spermine (tetramine), despite the stronger possibility of formation of intramolecular (N)H···:N and/or (C)H···:N bonds in these systems. In fact, it was verified that, in the solid, intramolecular interactions are overruled by intermolecular ones. Thus, the DFT calculations, carried out in the present work in view of helping the assignment of the vibrational patterns of the polyamines, were performed only for their linear, all-trans configuration. The homologous series of diamines, $H_2N(CH_2)_nNH_2$, exhibit C_{2h} symmetry for even values of *n*, while the molecules with $n =$ odd belong to the C_{2v} symmetry point group. Spermidine and spermine, in turn, display a much lower symmetry (C_1 and C_2, respectively). Both total geometry optimization and calculation of the harmonic vibrational frequencies and intensities were undertaken for the normal and the N-deuterated species (tables available from the authors upon request). The 6-31G* basis set was used systematically, after verifying that consideration of polarization functions on the hydrogen atoms did not pay for the 3-fold increase in computational requirements. As was seen in previous studies on similar systems,[20] DFT calculations carried out at the B3LYP/6-31G* level display a good correlation with the MP2/6-31G** results.

Both INS and Raman experiments were conducted on samples in the solid state. Deuteration of the samples saw the observation of the anticipated shifts to lower frequencies (in both INS and Raman) as well as the loss of some INS intensity for the bands assigned to the vibrational modes of the ND_2 group, as a consequence of the variations in both mass (frequencies) and scattering cross-section (INS intensities). In the INS spectra, this is clearly observed for the bands at ca. 1370 vs 1000 cm^{-1} (NH_2/ND_2 twisting modes) and at ca. 950 vs 730 cm^{-1} (NH_2/ND_2 wagging) (Figure 2). The most characteristic changes in the Raman pattern, in turn, are detected, as expected, for the amine torsional (ca. 390 vs 280 cm^{-1}), scissoring (ca. 1650 vs 1200 cm^{-1}), and stretching (ca. 3300 vs 2400 cm^{-1}, Figure 3) bands. Also, a wavenumber shift to lower energies is found (in both Raman and INS), in agreement with the theoretical results, for some of the LAM modes: those associated with a significant change in the CCN angle (Tables 1−6, Tables IS−VIS). In the

TABLE 8: LAM's for the Deuterated $D_2N(CH_2)_nND_2$ ($n = 2-10$, $n = 12$) Diamines, Spermidine-*N*-d_5 and Spermine-*N*-d_6

			i											
N			1	2	3	4	5	6	7	8	9	10	11	12
4	1,2dae	exp (INS)	439	317										
	(C_{2h})	exp (Raman)	436											
		calc[a]	411 (Ag)	249 (Bu)										
		κ	0.333	0.666										
5	1,3dap	exp (INS)	406	428										
	(C_{2v})	exp (Raman)	411	411	235									
		calc	375 (A1)	405 (B2)	171 (A1)									
		κ	0.250	0.500	0.750									
6	1,4dab	exp (INS)	359	486	319	169								
	(C_{2h})	exp (Raman)	359		324									
		calc	352 (Ag)	468 (Bu)	296 (Ag)	124 (Bu)								
		κ	0.200	0.400	0.600	0.800								
7	1,5dap	exp (INS)	301	483	438	278	142							
	(C_{2v})	exp (Raman)	320	477										
		calc	287 (A1)	474 (B2)	422 (A1)	242 (B2)	95 (A1)							
		κ	0.167	0.333	0.500	0.667	0.833							
8	1,6dah	exp (INS)	274	467	487	368	237	128						
	(C_{2h})	exp (Raman)	272		491									
		calc	261 (Ag)	458 (Bu)	477 (Ag)	343 (Bu)	193 (Ag)	77 (Bu)						
		κ	0.143	0.286	0.429	0.571	0.714	0.857						
9	1,7dah	exp (INS)	249	452	503	419	311		107					
	(C_{2v})	exp (Raman)	255			415	306							
		calc	232 (A1)	449 (B2)	497 (A1)	397 (B2)	290 (A1)	160 (B2)	60 (A1)					
		κ	0.125	0.250	0.375	0.500	0.625	0.750	0.875					
10	1,8dao	exp (INS)	231	401	504	487	381	262	167	112				
	(C_{2h})	exp (Raman)	229		500		388		165					
		calc	213 (Ag)	389 (Bu)	497 (Ag)	478 (Bu)	365 (Ag)	241 (Bu)	134 (Ag)	55 (Bu)				
		κ	0.111	0.222	0.333	0.444	0.555	0.666	0.777	0.888				
	spd	exp (INS)	239	395	511	494	382	267	163	94				
	(C_1)	exp (Raman)	233	397	509			274		92				
		calc	223	388	510	489	369	242	134	50				
		κ	0.111	0.222	0.333	0.444	0.555	0.666	0.777	0.888				
11	1,9dan	exp (INS)	213	375	491	506	436	325	235	154	99			
	(C_{2v})	exp (Raman)	227	373	494	510	429		213		93			
		calc	190 (A1)	369 (B2)	491 (A1)	500 (B2)	418 (A1)	310 (B2)	209 (A1)	109 (B2)	41 (A1)			
		κ	0.100	0.200	0.300	0.400	0.500	0.600	0.700	0.800	0.900			
12	1,10dad	exp (INS)	198	345	456	512	485	392	286	203	135	90		
	(C_{2h})	exp (Raman)	197		453		487		287		132			
		calc	177 (Ag)	336 (Bu)	445 (Ag)	511 (Bu)	488 (Ag)	382 (Bu)	274 (Ag)	177 (Bu)	94 (Ag)	37 (Bu)		
		κ	0.091	0.182	0.273	0.364	0.455	0.545	0.636	0.727	0.818	0.909		
14	1,12dad	exp (INS)	177	311	427	505	514	465	399	300	231	161	119	85
	(C_{2h})	exp (Raman)	173		427		516		400		231		123	
		calc	155 (Ag)	309 (Bu)	424 (Ag)	506 (Bu)	513 (Ag)	457 (Bu)	380 (Ag)	289 (Bu)	213 (Ag)	137 (Bu)	76 (Ag)	34 (Bu)
		κ	0.077	0.154	0.231	0.308	0.385	0.462	0.539	0.615	0.692	0.769	0.846	0.923
	sp	exp (INS)	174	318	432	522	522	479	398	318	240	158	114	75
	(C_2)	exp (Raman)	179		434	520	520		396		240	156	111	
		calc	165	316	432	527	518	469	384	295	215	135	71	26
		κ	0.077	0.154	0.231	0.308	0.385	0.462	0.539	0.615	0.692	0.769	0.846	0.923

[a] At the B3LYP/6-31G* level. $i = 1, 2, ..., (N - 2)$; $\kappa = i/(N - 1)$.

case of 1,10-diaminodecane, for instance, LAM 5, which is hardly detected in the Raman spectrum (very weak band close to LAM 3), is clearly observed in the N-deuterated amine, due to this shift to lower frequencies displayed by LAM 3 upon deuteration (Table VS).

The agreement between the INS experimental and calculated spectra showed to be rather good above 250 cm^{-1} (Figures 4 and 5), with the exception of the torsional modes of the amine terminal groups (discussed below).

A complete assignment of the LAM's for the whole series of homologous amines under study (including their N-deuterated forms) is given in Tables 7 and 8. This was carried out by comparison with the ab initio results and the analogous data obtained for the 5−25 *n*-alkanes.[23] It was verified that all the LAM's have the same INS intensity, their number increasing with chain length and the frequency of LAM 1 (accordion mode) being inversely proportional to this length (Tables 7 and 8, Figure 6).

The INS experimental LAM's observed for these polyamines are in good accordance with the LAM's of the corresponding *n*-alkanes[23] (Figure 7), which supports the idea of a significant conformational similarity (in the solid state) between these two sets of compounds. In the *n*-alkanes the CH_3 torsions appear as isolated and intense features around 250 cm^{-1} (e.g., Figure 7,

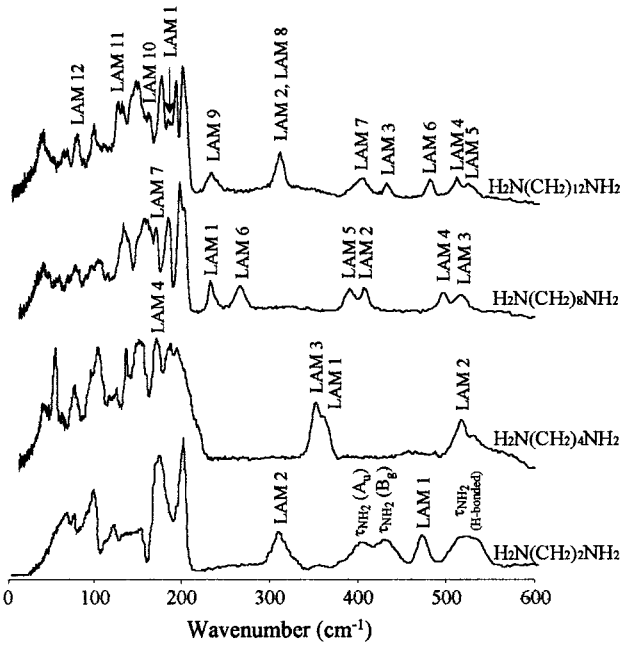

Figure 6. Experimental INS spectra (16−600 cm^{-1}, at 20 K) for some $H_2N(CH_2)_nNH_2$ diamines.

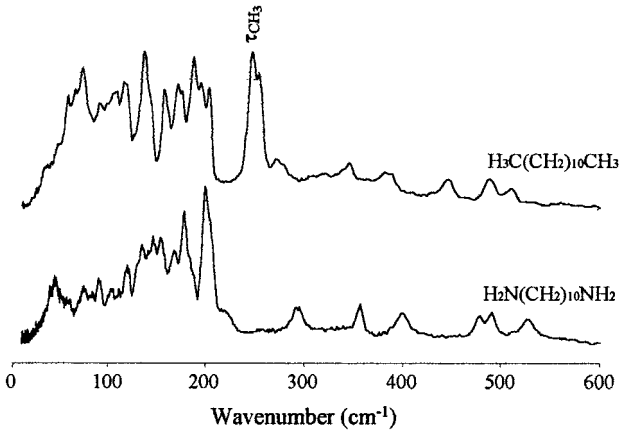

Figure 7. Experimental INS spectra (16−600 cm^{-1}, at 20 K) for a linear polyamine and the corresponding *n*-alkane.[23]

band at 247 cm^{-1}). They are best described as vibrations involving most of the alkane backbone and description in terms of the torsions of isolated CH_3 groups is inadequate. However, these vibrational modes obviously do not involve all of the CH_n units in the alkane; otherwise, the vibration would be part of the set of transverse modes in these systems, which appears below 200 cm^{-1}. In turn, in the polyamines studied (except for 1,2-diaminoethane) the torsional mode of the amine terminal groups is not clearly observed above 210 cm^{-1}, as would be expected from the theoretical calculations, which suggests that the occurrence of R−HN−H···NH_2−R intermolecular interactions completely changes the nature of that vibration, from a chain mode to a localized torsion, restricted to the NH_2 groups alone.

It should be stressed, however, that the nonobservation of the NH_2 torsion modes in INS, for most of the polyamines studied in the present work, constitutes an unexpected result. A possible explanation for this is now put forward. The fact that 1,2-diaminoethane appears as an exception, as both τ_{NH_2} A_u (409 cm^{-1}) and B_g (432 cm^{-1}) bands are distinctly detected (Figure 6) as well as a third band at 522 cm^{-1}, is interpreted considering the presence of dimers in the solid for this small molecule. In fact, 1,2-diaminoethane having such a short alkylic chain between the two amine terminal groups will not be prone to form polymeric structures, due to an inefficient electronic charge delocalization through the carbon skeleton upon formation of intermolecular H_2N···H interactions simultaneously in both ends of the molecule, the dimeric species being the most favorable one in the solid state. The three distinct INS features are thus assigned to the hydrogen-bonded (central) NH_2 groups (522 cm^{-1}) and to the (terminal) NH_2 moieties not engaged in intermolecular hydrogen close contacts (409 and 432 cm^{-1}). While the nondegeneracy of the lowest energy τ_{NH_2} modes is predicted, for this particular molecule alone, by the theoretical results ($\Delta\nu$ of 39 cm^{-1}, Table 1), the band at higher frequency is not found by the calculations. In the case of 1,3-diaminopropane and the larger diamines now investigated, in turn, oligomeric forms are probable to occur in the condensed phase, both NH_2 groups being thus involved in intermolecular hydrogen bonds, which would explain why only one band (H-bonded NH_2) is detected in the INS spectra (at ca. 530 cm^{-1}, for $H_2N(CH_2)_nNH_2$ $n = 3-5$, Tables 2−4). As the chain lengthtens, a clear and progressive intensity decrease of this feature is observed, until it completely disappears, for 1,6-diaminohexane (Table IS), due to the smaller and smaller relative weight of the amine hydrogens in the molecule (Figure 6). This hypothesis is corroborated by INS results obtained for similar linear

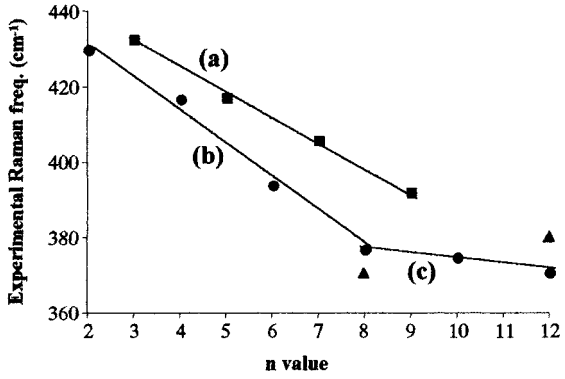

Figure 8. Plot of experimental Raman τ_{NH_2} frequencies vs chain length, for the series of polyamines studied: even-membered (●) and odd-membered (■) $H_2N(CH_2)_nNH_2$ diamines; spermidine and spermine (▲).

monoamines, according to which a weak τ_{NH_2} band is detected, for the shorter molecules only, at a frequency near to the one ascribed to the H_2N···H groups in the $H_2N(CH_2)_nNH_2$ systems discussed above (e.g., 525 cm^{-1} for *n*-propylamine).

Through analysis of the Raman spectra of the whole series of molecules it was verified that τ_{NH_2} displays a shift to lower frequencies as the polyamine increases, for the even- and odd-membered molecules, separately (Tables 1−6, Tables IS−VIS, Figure 8). This variation of the torsional oscillations of the chain can be explained by a loosening effect as it gets longer, which is clearly more significant for an increase in chain length from $n = 2$ to $n = 9$ (Figure 8, lines a and b). In fact, for the larger molecules studied, the shift to lower energies detected in the Raman spectra is much smaller (Figure 8, line c). This can be explained by the occurrence of intermolecular R−HN−H···NH_2−R close contacts at the terminal NH_2 groups of the chain. This type of interaction is present in some crystals,[42,43] one amine donating a proton to a neighbor and in turn accepting another proton from a third molecule. Actually, a clear shift of τ_{NH_2} to higher wavenumbers, when going from the liquid to the solid state, was previously observed in small primary amines[19,44] (e.g., 341 to 430 cm^{-1} for 1,2-diaminoethane[19]). This vibrational mode is, in fact, highly sensitive to intermolecular interactions, which are strongly dependent on the physical state of the sample, varying in the order: gas (isolated molecule) ≪ liquid < solid. Also, it was now verified that this shift to higher energies decreases considerably as the polyamine chain lengthens (as described above), due to a weakening of the top-to-top close contacts between neighboring molecules as the number of carbons increase. The observed *n*-even/*n*-odd dependence of the τ_{NH_2} mode (Figure 8, lines a and b) may, in turn, be due to changes in their crystal structure with the parity of the molecules, similarly to what has been previously recognized for *n*-alkanes[45,46] (namely the tighter packing of the even-membered chains relative to the odd-membered ones).

For the N-deuterated molecules, no significant wavenumber changes were detected for the amine torsional mode (Tables 1−6, Tables IS−VIS), probably due to the weaker R−DN−D···ND_2−R intermolecular interactions. However, the τ_{ND_2} Raman bands for odd-membered molecules are consistently observed at ca. 15 cm^{-1} higher frequencies relative to the even-membered ones. Moreover, a shift of ca. 100/50 cm^{-1} to lower frequencies is detected between the observed and calculated Raman τ_{NH_2}/τ_{ND_2} wavenumbers, respectively. Also, the τ_{NH_2} steady displacement associated with the increase of the polyamine chain (Figure 8) is not predicted by the theoretical calculations. In fact, the vibrational consequences of the intermolecular hydrogen bonds occurring in this kind of systems cannot be

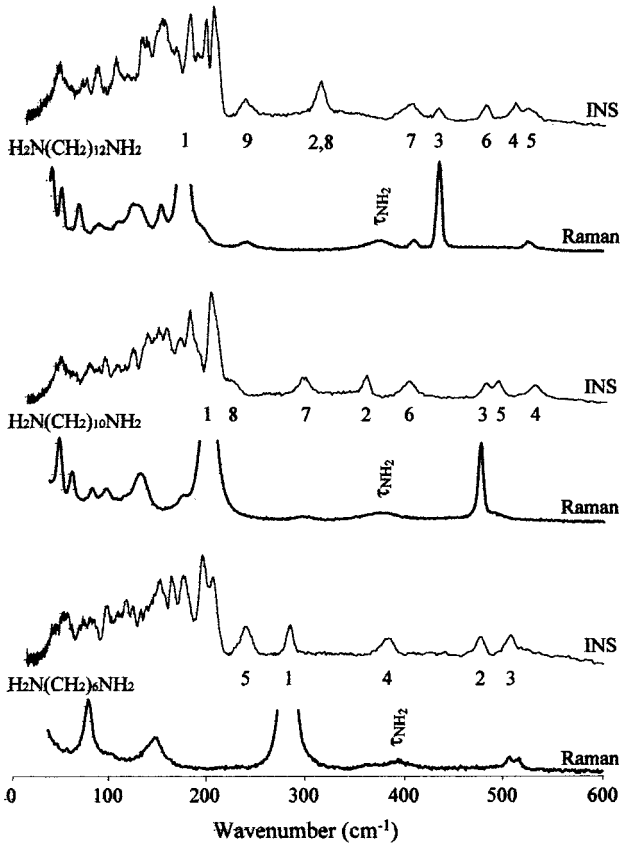

Figure 9. Experimental Raman and INS spectra (low-frequency region) for some $H_2N(CH_2)_nNH_2$ diamines. (the numbers refer to the corresponding LAM modes).

captured by the isolated-molecule calculations used along the present study, which readily explains the above-mentioned discrepancies between calculated and experimental data.

A further consequence of the presence of H-bonding is the lowering of the N−H stretching modes and the concomitant wavenumber increase of the C−N−H deformations. This is quite a typical amine behavior and has been repeatedly reported for small, linear amines, for both the terminal and central nitrogen atoms[14,19,47,48] (namely when going from the liquid to the solid state) and corroborates the results now obtained for the larger polyamines.

When the experimental INS and Raman data are compared (Figure 9), it is easily verified that while all the LAM's are detected by INS, in the Raman spectra, only the first LAM band is distinctly observed for all the polyamines studied. In fact, most of the higher number LAM's are either very weak or symmetry forbidden transitions in Raman spectroscopy. As the molecules get larger, however, more LAM's are progressively detected and the ones with the same number of nodes become more and more distinct (e.g., LAM 3, Figure 9).

4. Conclusions

The complementary use of both Raman and INS spectroscopies in the present work allowed the assignment of all the LAM's for the polyamines studied ($H_2N(CH_2)_nNH_2$ ($n = 2-10$ and $n = 12$), spermidine and spermine) both for their undeuterated and N-deuterated forms. In fact, INS is very useful for the analysis of the frequency range below 600 cm^{-1}, where it displays a clear and intense vibrational pattern, while above around 1800 cm^{-1} its spectral quality begins to deteriorate. Raman spectroscopy comes into its own again in this region, thus being particularly useful for the analysis of CH and NH/ND stretching modes.

For the linear polyamines under study, the lowest energy conformation, in the solid state, was found to be the all-trans one. The DFT calculations performed at the B3LYP/6-31G* level adequately mimicked this kind of systems, leading to a particularly good agreement between the calculated and experimental spectra. This allowed a confident assignment of the observed Raman and INS patterns.

The present study contributes to a better understanding of the conformational behavior of linear polyamines, which, in the solid state, is strongly determined by the occurrence of intermolecular R−HN−H···NH_2−R hydrogen-type interactions, mainly at the terminal NH_2 groups of the chains. This kind of close contact was found to give rise either to infinite chain polymeric forms or to dimeric species, in the case of 1,2-diaminoethane.

The knowlegde of the structural preferences of biogenic polyamines is of utmost importance for the design of complexes displaying this kind of molecule as linkers between metal centers (e.g., Pt(II) or Pd(II)), which have been found to act as rather efficient anticancer agents (often even overcoming the cytotoxic effect of the drugs under clinical use).

Acknowledgment. M.P.M. and L.A.B.C. acknowledge financial support from the Portuguese Foundation for Science and Technology, Project PBIC/C/QUI/2219/95. We thank Prof. B. S. Hudson and Dr. Chris Middleton (Syracuse University, Syracuse, NY) for help and discussions on the calculation of the INS spectra from ab initio results.

Supporting Information Available: Tables comprising Raman and INS experimental and calculated wavenumbers for the diamines $H_2N(CH_2)_nNH_2$ ($n = 6-10$, $n = 12$), in the low-frequency region, as well as corresponding assignments. This material is available free of charge via the Internet at http://pubs.acs.org.

References and Notes

(1) Pegg, A. E. *Cancer Res.* **1988**, *48*, 759.
(2) Heby, O.; Persson, L. *Trends Biochem. Sci.* **1990**, *15*, 153.
(3) Tamori, A.; Nishiguchi, S.; Kuroki, T.; Koh, N.; Kobayashi, K.; Yano, Y.; Otani, S. *Cancer Res.* **1995**, *55*, 3500.
(4) Auvinen, M.; Passinen, A.; Anderson, L. C.; Holtta, E. *Nature* **1992**, *360*, 355.
(5) Janne, J.; Alhonen, L.; Linonen, P. *Ann. Med.* **1991**, *23*, 241.
(6) Nishioka, K. *Polyamines in Cancer: Basic Mechanisms and Clinical Approaches*; Springer-Verlag: Germany, 1966.
(7) O'Brien, T. G.; Megosh, L. C.; Gilliard, G.; Soler, A. P. *Cancer Res.* **1997**, *57*, 2630.
(8) Porter, C. W.; Sufrin, J. R. *Anticancer Res.* **1986**, *6*, 525.
(9) Porter, C. W.; Bergeron, R. J. *Progress in Polyamine Research*; Plenum: New York, 1988.
(10) Auvinen, M.; Paasinen, A.; Anderson, L. C.; Holtta, E. *Nature* **1992**, *360*, 355.
(11) Moshier, J. A.; Dosescu, J.; Skunca, M.; Luk, G. D. *Cancer Res.* **1993**, *53*, 2618.
(12) O'Brien, T. G.; Megosh, L. C.; Gilliard, G.; Soler, A. P. *Cancer Res.* **1997**, *57*, 2630.
(13) Rauter, H.; Di Domenico, R.; Menta, E.; Oliva, A.; Qu, Y.; Farrell, N. *Inorg. Chem.* **1997**, *36*, 3919 and references therein.
(14) Batista de Carvalho, L. A. E.; Amorim da Costa, A. M.; Duarte, M. L.; Teixeira-Dias, J. J. C. *Spectrochim. Acta* **1988**, *44A*, 723.
(15) Batista de Carvalho, L. A. E.; Amorim da Costa, A. M.; Teixeira-Dias, J. J. C. *J. Mol. Struct. (THEOCHEM.)* **1990**, *205*, 327.
(16) Batista de Carvalho, L. A. E.; Teixeira-Dias, J. J. C.; Fausto, R. *Struct. Chem.* **1990**, *1*, 533.
(17) Bertoluzza, A.; Fagnano, C.; Finelli, P.; Morelli, M. A.; Simoni, R.; Tosi, R. *J. Raman Spectrosc.* **1983**, *14*, 386.
(18) Ghazanfar, S. A. S.; Edsall, J. T.; Myers, D. V. *J. Am. Chem. Soc.* **1964**, *86*, 559.

(19) Batista de Carvalho, L. A. E.; Lourenço, L. E.; Marques, M. P. M. *J. Mol. Struct.* **1999**, *482*−*483*, 639 and references therein.
(20) Batista de Carvalho, L. A. E.; Marques, M. P. M. Unpublished results.
(21) Marques, M. P. M.; Batista de Carvalho, L. A. E. *COST 917: Biogenically Active Amines in Food*; Morgan, D. M. L., White, A., Sánchez-Jiménez, F., Bardocz, S., Eds.; European Comission: Luxemburg, 2000; Vol. IV, p 122.
(22) Parker, S. F.; Braden, D. A.; Tomkinson, J.; Hudson, B. S. *J. Phys. Chem. B* **1998**, *102*, 5955.
(23) Braden, D. A.; Parker, S. F.; Tomkinson, J.; Hudson, B. S. *J. Chem. Phys.* **1999**, *111*, 429.
(24) www.isis.rl.ac.uk.
(25) Frisch, M. J.; Trucks, G. W.; Schlegel, H. B.; Scuseria, G. E.; Robb, M. A.; Cheeseman, J. R.; Zakrzewski, V. G.; Montgomery, J. A., Jr.; Stratmann, R. E.; Burant, J. C.; Dapprich, S.; Millam, J. M.; Daniels, A. D.; Kudin, K. N.; Strain, M. C.; Farkas, O.; Tomasi, J.; Barone, V.; Cossi, M.; Cammi, R.; Mennucci, B.; Pomelli, C.; Adamo, C.; Clifford, S.; Ochterski, J.; Petersson, G. A.; Ayala, P. Y.; Cui, Q.; Morokuma, K.; Malick, D. K.; Rabuck, A. D.; Raghavachari, K.; Foresman, J. B.; Cioslowski, J.; Ortiz, J. V.; Stefanov, B. B.; Liu, G.; Liashenko, A.; Piskorz, P.; Komaromi, I.; Gomperts, R.; Martin, R. L.; Fox, D. J.; Keith, T.; Al-Laham, M. A.; Peng, C. Y.; Nanayakkara, A.; Gonzalez, C.; Challacombe, M.; Gill, P. M. W.; Johnson, B. G.; Chen, W.; Wong, M. W.; Andres, J. L.; Head-Gordon, M.; Replogle, E. S.; Pople, J. A. *Gaussian 98*, revision A.3; Gaussian, Inc.: Pittsburgh, PA, 1998.
(26) Russo, T. V.; Martin, R. L.; Hay, P. J. *J. Phys. Chem.* **1995**, *99*, 17085.
(27) Ignaczak, A.; Gomes, J. A. N. F. *Chem. Phys. Lett.* **1996**, *257*, 609.
(28) Cotton, F. A.; Feng, X. *J. Am. Chem. Soc.* **1997**, *119*, 7514.
(29) Wagener, T.; Frenking, G. *Inorg. Chem.* **1998**, *37*, 1805.
(30) Ignaczak, A.; Gomes, J. A. N. F. *J. Electroanal. Chem.* **1997**, *420*, 209.
(31) Cotton, F. A.; Feng, X. *J. Am. Chem. Soc.* **1998**, *120*, 3387.
(32) Lee, C.; Yang, W.; Parr, R. G. *Phys. Rev.* **1988**, *B37*, 785.
(33) Miehlich, B.; Savin, A.; Stoll, H.; Preuss, H. *Chem. Phys. Lett.* **1989**, *157*, 200.
(34) Becke, A. *Phys. Rev.* **1988**, *A38*, 3098.
(35) Becke, A. *J. Chem. Phys.* **1993**, *98*, 5648.
(36) Hariharan, P. C.; Pople, J. A. *Theor. Chim. Acta* **1973**, *28*, 213.
(37) Francl, M. M.; Pietro, W. J.; Hehre, W. J.; Binkley, J. S.; Gordon, M. S.; DeFrees, D. J.; Pople, J. A. *J. Chem. Phys.* **1982**, *77*, 3654.
(38) Peng, C.; Ayala, P. Y.; Schlegel, H. B.; Frisch, M. J. *J. Comput. Chem.* **1996**, *17*, 49.
(39) Mirkin, N. G.; Krimm, S. *J. Phys. Chem.* **1993**, *97*, 13887 and references therein.
(40) Taylor, R.; Kennard, O. *J. Am. Chem. Soc.* **1982**, *104*, 5063.
(41) Steiner, T. *Chem. Commun.* **1997**, 727.
(42) Giglio, E.; Liquori, A. M.; Puliti, R.; Ripamonti, A. *Acta Crystallogr.* **1966**, *20*, 652.
(43) Giglio, E.; Liquori, A. M.; Puliti, R.; Ripamonti, A. *Acta Crystallogr.* **1966**, *20*, 683.
(44) Batista de Carvalho, L. A. E. Ph.D. Thesis, Coimbra, 1990.
(45) Mathisen, H.; Norman, N.; Pedersen, B. F. *Acta Chim. Scand.* **1967**, *21*, 127.
(46) Barnes, J.; Franconi, B. *J. Phys. Chem. Ref. Data* **1978**, *7*, 1309 and references therein.
(47) Colthup, N. B.; Daly, L. H.; Wiberley, S. E. *Infrared and Raman Spectroscopy*, 2nd ed.; Academic Press: New York, 1975; pp 216−219.
(48) Batista de Carvalho, L. A. E.; Teixeira-Dias, J. J. C. *J. Raman Spectrosc.* **1995**, *26*, 653.